

MEASUREMENT OF MULTIPLE MUON RATES UNDERGROUND

G. H. Lowe*, H. E. Bergeson, J. W. Keuffel,
 V. D. Sandberg, and S. Ozaki†
 Department of Physics, University of Utah
 Salt Lake City, Utah (USA) 84112

New and more extensive data on multiple muons underground are presented as rates for various multiplicities in a fiducial plane of 80 m^2 . The results are in agreement with the scaling model calculations of Elbert and Mason in the range 10-1000 TeV.

1. Introduction. The advent of the NAS and ISR machines, together with recent theoretical developments of limiting fragmentation and scaling, make it especially interesting now to look for cosmic ray measurements sensitive to the detailed features of the models of hadronic interactions under consideration. The multiple muons observed deep underground offer special promise in this regard, for they carry rather direct information about the particles produced in the earliest stages, often from the very first collision, in the hadronic cascade produced by a cosmic ray primary. Their interpretation is greatly facilitated by the scaling theory, which provides a framework against which the observations may be tested. The framework is anchored by accelerator results near 1 TeV and scaling provides a clear prescription for extrapolation to cosmic ray energies. Deviations from the scaling prediction, should there be any, may then be interpreted in terms of the onset of some new phenomena.

However, the predictions depend not only on the collision model, but also on the spectrum and composition assumed for the primaries. The degree to which the spectrum effects can be separated out from the effects of the collision model is not yet fully known, although the richness of the multiple muon data, together with the availability of some information from other sources about the spectrum, hold out hope that the separation can be carried out.

In this paper, we describe the techniques whereby the multiple muons are studied with the Utah cosmic ray detector and summarize results obtained to date with an expanded, 80 m^2 fiducial plane. Earlier work (Davis et al 1971) had been limited to a restricted area of the detector much smaller for the most part than 80 m^2 . Comparisons with scaling predictions are given in the paper by Elbert and Mason (1973) scheduled for a combined HE-NN session of this conference. Implications of the results for the spectrum and composition of the primaries are reported in a paper by Elbert and Morrison (1973) in the OG session of this conference. It should be emphasized that both the calculations and the methods of treating the experimental data are still in a preliminary state.

2. Information Carried by Multiple Muons Underground. In order to see how muons observed in the Utah detector may be used to study the properties of hadronic collisions high in the atmosphere, it is useful to consider the schematic diagram shown in Fig. 1. A primary (say a proton of 10^{15} eV) strikes the top of the atmosphere and initiates a hadronic cascade. Pions (and kaons) in the cascade may decay to produce muons, the decay probability being $PD \sim (90 \text{ GeV}/E\pi) \sec \theta$ at one interaction length down into the atmosphere and

inversely as the density of the air at lower levels. The rock above the Utah detector acts as a muon range analyzer; by looking in different directions, muon energy thresholds from 0.5 to 20 TeV may be imposed.

The quantities actually observed are (a) the rates $J(n_D, h, \theta)$ of events where n_D muons traverse the 80 m^2 fiducial area of the detector at a slant depth h and a zenith angle θ , and (b) the mean separation $x_0(h, \theta)$ of the muons. (Later we expect to study also the geomagnetic separation of the muons, important for long flight paths at large zenith angles, and the details of the distribution in separations of muons for various n_D .)

Ideally, one would like to extract from the observed quantities information about the basic parameters of the collision model: the total cross section, the multiplicity, the distribution in longitudinal momentum of the produced particles, and the transverse momentum, all as a function of the primary energy. The muons observed come, of course, from a random sample of the produced pions and kaons, and it is necessary to investigate with the aid of a Monte Carlo calculation the degree to which this sample is sensitive to the assumed hadronic collision model.

The median primary energies giving rise to events with a given n_D and h have been calculated by Elbert and Mason (1973) on the basis of the scaling model and the assumption of primary protons with a differential spectral index of 2.7. The results of the calculations are given in Table I. One may note

TABLE I. Median primary energies giving rise to multiple muon events.

Depth 10^5 g/cm^2	Median Primary Energies (TeV)				
	$n_D = 1$	2	3	4	5
2.4	10	76	350	870	950
3.2	15	125	900	2300	
4.8	31	220			
7.2	63				
10.0	137				

that the effects of a primary particle of a given energy appear as singles ($n_D = 1$) at a particular depth and as higher multiples at successively shallower depths, as might be expected from Fig. 1. The Monte Carlo calculations also show that the median x -values for the parents of the muons in events with $n_D = 5$ is 0.10, as against 0.23 for singles. The calculations further confirm that a considerable fraction of the muons in the low-multiplicity events come from the first or second collisions of the primary (90% for singles, 79% for doubles, in one example). This desirable state of affairs is in large part a consequence of the very large detector, whose dimensions are of the order of the shower radius; for otherwise a small n_D could still be associated with a very large number of muons underground, and hence, with the cascading effects of

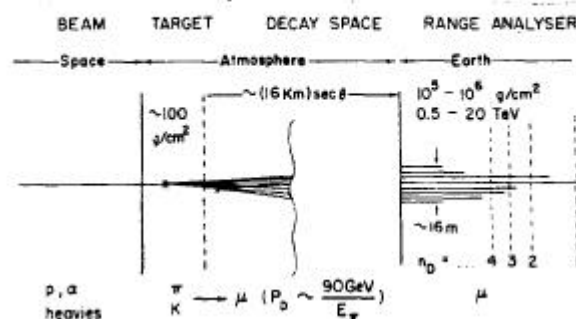


Fig. 1. Schematic diagram of the high energy muon component of an energetic cosmic ray event.

successive generations of collisions. The cascade effects tend to wash out the details of the original high-energy collision.

The calculations have not yet been extended to the point where definite statements about the sensitivity of the multiple muon phenomena to the total cross section and the multiplicity can be made. However, the shower spread does appear to yield an accurate measure of the transverse momentum.

3. Apparatus and Analysis. The detector has been described in some detail (Bergeson *et al* 1967, Cassidy *et al* 1973, Hilton *et al* 1967, Keuffel *et al* 1967). Briefly, it consists of 600 cylindrical spark counters arrayed in 15 vertical planes, each $6 \times 10 \text{ m}^2$, as shown in Fig. 2. A trigger is provided by water-filled Cherenkov counters. The spark counters resemble oversized Geiger counters, 15 cm dia. x 10 m long, but operated in a pulsed mode at a higher pressure so that the discharge is a sharply localized corona spike which is detected by means of a sonic ranging system.

A computer pattern recognition program is used. The efficiency of the recognition program ranges from greater than 99% for events which contain 1 muon in the detector to 85-90% for events which contain 5 muons in the detector.

The actual area of the detector perpendicular to muons which pass through three or more groups of spark counters varies considerably in both size and shape as the zenith and azimuth angles of incoming muons are varied. However, the Cherenkov triggering walls of the detector, when projected into a plane perpendicular to the direction of travel of the muons in an event, form a figure which is fairly constant in area and shape. The mean area of this figure is somewhat greater than 80 m^2 . With muons which pass through only two groups of spark counters accepted in the analysis (the pattern recognition program picks up greater than 90% of the two group muons which are parallel to a three group muon) only small parts of the figure are insensitive to a through-going muon.

All muons in an event are required to pass through an imaginary plane of area 80 m^2 independent of angle which is superimposed upon the detector. If this "superplane" were sensitive over its entire area, the acceptance criteria for all events would be the same for the same size steradian bin. However, there are insensitive holes in the superplane for which corrections to the above simple aperture must be made.

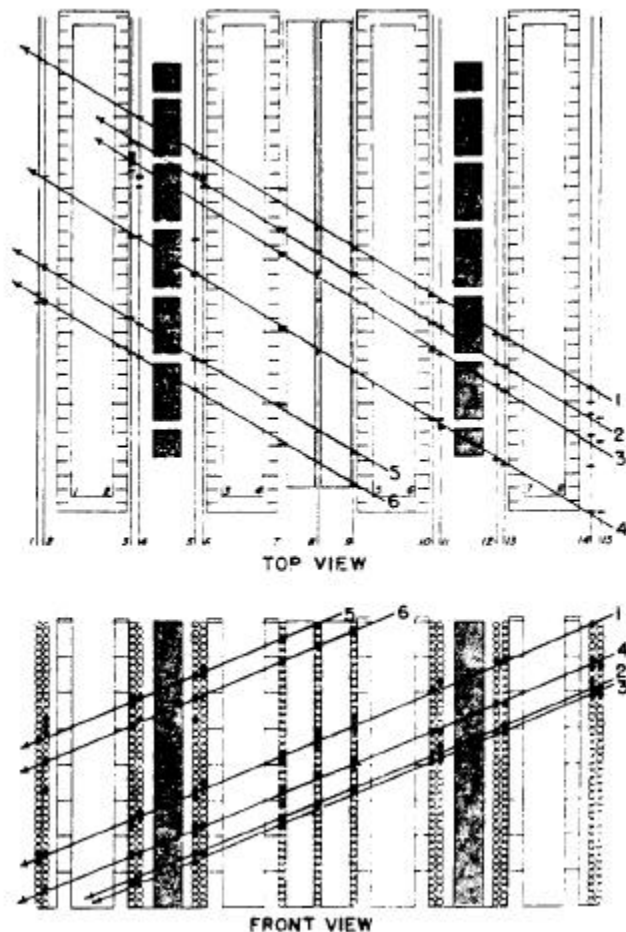


Fig. 2. Plot of an event containing 6 muons. The coordinates of the sparks in the top view are obtained from the time delays of the acoustical pulses.

The corrections to the aperture are made assuming muons in events on the average are distributed uniformly over the detector. The allowable size of the correction is kept small for all data used. Tests of intensity vs. size of the correction made for the data have disclosed no discernable effect.

The rates were corrected for the measured detector triggering efficiency. As the number of muons passing through the detector in an event increases, the average amount of light in each Cherenkov tank increases and the triggering efficiency of the detector approaches 100%. Thus, efficiency measurements for events having more than one muon in the detector were not nearly the problem that they were for events containing a single muon in the 1969 data (approximately 5% error for singles).

4. Results. The results are presented in the form of rates $J(n_D, h, \theta)$, which represent the number of events per second per steradian containing exactly n_D muons within the superplane area of 80 m^2 at zenith angle θ and slant depth h . Note that the usual muon intensity as measured by small detectors is given by $I(h, \theta) = \bar{O} n_D J(n_D, h, \theta) / 80 \text{ m}^2$.

Table II gives the total number of events of each multiplicity in the 1969 data for a running time of 1.8×10^7 sec. Since the data are scattered

TABLE II. Number of events of different multiplicities.

Multiplicity	1	2	3	4	5	6	7	8	9	10
Number	176,805	12,016	2,645	928	402	190	100	40	18	8

over a wide range of depths and zenith angles, it is necessary to consolidate them in some way in order to put the results in a tractable form. The first step in this procedure is to study the depth dependence of the rates. Rates at fixed θ and n_D were fit as a function of depth. This function of depth in turn was used to center the data in 800 hg/cm^2 bins in order to look at the θ dependence of the rates.

An example of the dependence of the rates on angle is given in Fig. 3. The increase in muon decay probability with $\sec \theta$ is approximately compensated by the decrease in muon density with $\sec \theta$.

Table III summarizes the data at two angles, $\theta = 47.5^\circ$, and $\theta = 62.5^\circ$.

The data in the present experiment were taken in 1969, but include many more events because of the 80 m^2 fiducial area. Data taken in 1971-72 agrees within error flags with the 1969 data, but the analysis of the 1971-72 data is not yet complete.

Measurements have been published for the mean separation $x_0(h, \theta)$ (Davis et al 1971, Coats et al 1970) when analyzed in the form of a decoherence curve. The decoherence curve is defined to be the counting rate per second per steradian of a pair of 1 m^2 detectors operated in coincidence as a function of their separation. The decoherence rates fit an exponential dependence over the range of separations up to 11 m, and the mean separation $x_0(h, \theta)$ are taken from these fits. Typical values from the 1969 data are given in the paper by Elbert and Mason (1973) in the combined HE-MN session of this conference. Again the analysis of the 1971-72 data is not yet complete.

5. Discussion. Pioneering calculations for the interpretation of multiple muon phenomena were done prior to the advent of scaling by the Durham group under Wolfendale (Adcock *et al* 1971). Their calculations were based on an $E_p^{1/4}$ power law for pion multiplicity produced in the primary-air collision. Comparison of their calculations with the observed ratios of doubles rates divided by singles, and triples rates divided by singles seems to indicate a necessity for a $\langle P_T \rangle$ which increases from somewhat less than 0.5 GeV/c at 2400 hg/cm² to greater than 1 GeV/c at greater than 4800 hg/cm². On the other hand, comparison of the observed decoherence curves with the calculations did not call for such an increase, giving an inconsistency at the one standard deviation level.

Comparisons with the scaling model are given in the paper by Elbert and Mason (1973) in the combined HE-MN session of this conference. The observations and calculations show reasonable agreement over the energy range 10-1000 TeV primary energy.

Conclusions about the spectrum and composition are reported in the paper by Elbert *et al* (1973) in the OG session of this conference.

Acknowledgements. This research was supported by the National Science Foundation.

References.

- *This paper contains the main results of the Ph.D. thesis of George H. Lowe, University of Utah, 1973.
- †Permanent address: Osaka City University, Osaka, Japan.
- Adcock, C. *et al* 1970, J. Phys. A: Gen. Phys., 4, 276.
- Bergeson, H. E. and Wolfson, C. J. 1967, Nucl. Inst. and Meth. 51, 47.
- Cassiday, G. L., Groom, D. E. and Larson, M. O. 1973, Nucl. Inst. and Meth. 107, 509.
- Coats, R. B. *et al* 1970, J. Phys. A: Gen. Phys. 3, 689.
- Davis, K. H. *et al* 1971, Phys. Rev. D, 4, 607.
- Elbert, J. W. and Mason, G. W., Paper 389, HE-MN session of this conference.
- Elbert, J. W. *et al* Paper 371, OG session of this conference.
- Hilton, L. K. *et al* 1967, Nucl. Inst. and Meth. 51, 43.
- Keuffel, J. W. and Parker, J. L. 1967, Nucl. Inst. and Meth. 51, 29.

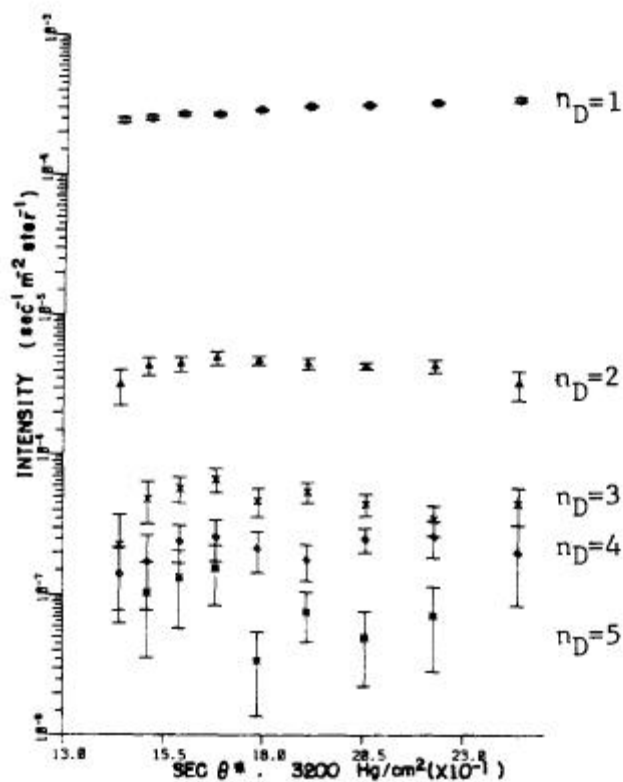


Fig. 3. Example of g dependence of rates. Ordinate is in intensity ($J(n_D, e, h)/80 \text{ m}^2$), abscissa in sece.

TABLE III. Entries are rates $J(n_D, \theta, h)$ with errors (including estimated systematics).

Depth $\times 10^5$ g/cm ²	$n_D = 1$	2	3	4	5	6	7	8
A. $\theta = 47.5^\circ$								
2.4	7.75×10^{-2} $\pm .11 \times 10^{-2}$	1.34×10^{-3} $\pm .1 \times 10^{-4}$	1.58×10^{-4} $\pm .25 \times 10^{-5}$	4.7×10^{-5} $\pm .5 \times 10^{-6}$	2.2×10^{-5} $\pm .3 \times 10^{-6}$	1.0×10^{-5} $\pm .2 \times 10^{-6}$	6.0×10^{-6} $\pm .2 \times 10^{-6}$	3.2×10^{-6} $\pm .6 \times 10^{-6}$
3.2	2.10×10^{-2} $\pm .04 \times 10^{-2}$	3.4×10^{-4} $\pm .4 \times 10^{-5}$	3.7×10^{-5} $\pm .9 \times 10^{-6}$	1.3×10^{-5} $\pm .3 \times 10^{-6}$	4.0×10^{-6} $\pm 1.0 \times 10^{-6}$	3.2×10^{-6} $\pm 1.6 \times 10^{-6}$	2.4×10^{-6} $\pm 1.6 \times 10^{-6}$	
B. $\theta = 62.5^\circ$								
3.2	2.91×10^{-2} $\pm .04 \times 10^{-2}$	3.36×10^{-4} $\pm .2 \times 10^{-5}$	3.4×10^{-5} $\pm .5 \times 10^{-6}$	1.7×10^{-5} $\pm .3 \times 10^{-6}$	No angular dependence observed, approximately the same as the values at 47.5° .			
4.0	9.01×10^{-3} $\pm .16 \times 10^{-3}$	1.1×10^{-4} $\pm .2 \times 10^{-5}$	1.5×10^{-5} $\pm .3 \times 10^{-6}$	4.8×10^{-6} $\pm 1.2 \times 10^{-6}$	2.4×10^{-6} $\pm .8 \times 10^{-7}$	8.0×10^{-7} $\pm 6.0 \times 10^{-7}$		
4.8	3.7×10^{-3} $\pm .3 \times 10^{-3}$	3.4×10^{-5} $\pm .6 \times 10^{-6}$	4.4×10^{-6} $\pm 1.2 \times 10^{-6}$	3.0×10^{-6} $\pm 2.0 \times 10^{-6}$				
5.6		1.5×10^{-5} $\pm .4 \times 10^{-6}$	2.8×10^{-6} $\pm 1.0 \times 10^{-6}$	8.0×10^{-7} $\pm 5.0 \times 10^{-7}$	No data points at 62.5° , interpolated as flat with θ .			

Filename: icrc733-1878
Directory: C:\WINDOWS\Desktop\Amy's Papers
Template: C:\Program Files\Microsoft Office\Templates\Normal.dot
Title:
Subject:
Author:
Keywords:
Comments:
Creation Date: 07/21/01 6:48 PM
Change Number: 3
Last Saved On: 08/21/01 12:47 PM
Last Saved By: user
Total Editing Time: 48 Minutes
Last Printed On: 10/08/01 11:32 AM
As of Last Complete Printing
Number of Pages: 6
Number of Words: 1,945 (approx.)
Number of Characters: 11,092 (approx.)